


[View Journal Online](#)
[View Article Online](#)

Crystallographic identification of a novel 2,4,5-tri(*N*-methyl-4-pyridinium)-1,3-thiazole with a complex network of polyiodide/iodine counter ions and co-crystallized cyclododecasulfur (S₁₂)

 Ibukun Oluwaseun Shotonwa ^{1,*} and René T. Boeré ²
¹ Department of Chemistry, Lagos State University, Ojo, Lagos, 102101, Nigeria
 ibukun.shotonwa@lasu.edu.ng (I.O.S)

² Department of Chemistry and Biochemistry, University of Lethbridge, 4401 University Drive West, Lethbridge, Alberta, T1K3M4, Canada
 boere@uleth.ca (R.T.B.)

 * Corresponding author at: Department of Chemistry, Lagos State University, Ojo, Lagos, 102101, Nigeria.
 e-mail: ibukun.shotonwa@lasu.edu.ng (I.O. Shotonwa).

RESEARCH ARTICLE



doi 10.5155/eurjchem.12.2.179-186.2108

Received: 01 February 2021

Received in revised form: 26 March 2021

Accepted: 05 April 2021

Published online: 30 June 2021

Printed: 30 June 2021

KEYWORDS

 Sulfur
 Iodine
 1,3-Thiazole
 Sulfur heterocycles
 Crystal engineering
 Single crystal structure

ABSTRACT

The crystals of an unprecedented 2,4,5-tri(*N*-methylpyridinium)-1,3-thiazole are monoclinic and belong to the space group *P*2₁/*c* as determined by single-crystal XRD. Crystal data for C₂₁H₂₁I₁₃N₄S_{5.98}: monoclinic, *a* = 7.5627(5) Å, *b* = 30.6764(19) Å, *c* = 20.8848(15) Å, β = 91.632(6)°, *V* = 4843.2(6) Å³, *Z* = 4, *T* = 100.01(10) K, μ(Cu Kα) = 67.840 mm⁻¹, *D*_{calc} = 2.977 g/cm³, 17906 reflections measured (7.152° ≤ 2θ ≤ 162.94°), 17906 unique (*R*_{sigma} = 0.0607) which were used in all calculations. The final *R*₁ was 0.1366 [*I* > 2σ(*I*)] and *wR*₂ was 0.3926 (all data). The crystal lattice contains 2,4,5-tri(*N*-methylpyridinium)-1,3-thiazole, molecular iodine and triiodide counterions which interact with one another to coordinatively form polyiodides, as well as a surprising co-crystallized neutral molecule of cyclododecasulfur (S₁₂). Close monitoring of the synthetic procedure reveals chemical condensation and decomposition of the thioamide reagent to be the impetus for the formation of individual components of the crystal lattice. Analysis of the XRD, including a Hirshfeld surface analysis, shows that (a) the crystal lattice has a number of stabilizing Coulombic short contacts such as I⋯I, I⋯S, I⋯C, and C⋯S and non-classical C-H⋯I and C-H⋯S hydrogen bond interactions (b) the iodine/iodide network are major determinants in the stability of its crystal lattice despite the reduced occupancies of sulfur and (c) the Hirshfeld analysis in comparison with the conventional Mercury visualization program was able to simplify, identify and quantify complex atom-atom interactions such as H⋯H and N⋯I in its crystal lattice. Herein, it is reported, for the first time, the formation of co-crystallized, neutral cyclododecasulfur (S₁₂) from thioamide as the sulfur source. S₁₂ displays a consistent geometry and comparable average S-S distances, S-S-S angles and torsion angles with previously reported crystal structures of S₁₂. The complex network facilitated by the formation of polyiodides via the interaction of symmetric and asymmetric triiodides and iodine has resulted in quite strong interactions that are less than the sums of the van der Waals radii of two connected atoms as well as an array of fascinating geometrical alignments such as T-shape, trigonal pyramidal and L-shape.

 Cite this: *Eur. J. Chem.* 2021, 12(2), 179-186

 Journal website: www.eurjchem.com

1. Introduction

2,4,5-trisubstituted-1,3-thiazoles form a class of stable S/N containing heterocycles with extensive synthetic details [1] and notable applications in areas such as biology, pharmacy and photochemistry [2-6]. They also have detailed coordination chemistry with a wide variety of solid-state structural information and applications [7,8].

The complex interaction of iodine with unsaturated nitrogen-containing heterocycles has been reported to yield quite a number of salts and charge transfer complexes with interesting 3D features [9]. The driving forces for their fascinating properties are the presence of iodine, a solid-state structure-controlling vector which has the ability to condense heterocycles into ionic species with the eventual crystallization

into polyiodides; very iodine-rich complexes formed from an equilibrium-driven coordination of triiodide anions with iodine molecules [10-14].

Elemental sulfur has the highest number of solid-state allotropes of any element in the periodic table, which range from unbranched cyclic molecules with ring sizes 6-20, to polymeric chains of random coils and helical conformations. A detailed review of sulfur's allotropes with focus on their physical and chemical properties, preparation, characterization, crystal structures, and computational analyses is available [15].

Following on our previous report on the synthesis and structure of 1-methyl-4-thiocarbamoylpyridin-1-ium iodide [16], we herein report the synthesis, solid-state structural characterization and analysis of compound **1**, a novel and

Table 1. Crystal data and structure refinement for structure 1.

Parameter	Value
Empirical formula	C ₂₁ H ₂₁ I ₁₃ N ₄ S _{5.98}
Formula weight	2170.84
Temperature (K)	100.01(10)
Crystal system	Monoclinic
Space group	P2 ₁ /c
a (Å)	7.5627(5)
b (Å)	30.6764(19)
c (Å)	20.8848(15)
α (°)	90
β (°)	91.632(6)
γ (°)	90
Volume (Å ³)	4843.2(6)
Z	4
ρ _{calc} (g/cm ³)	2.977
μ (mm ⁻¹)	67.840
F(000)	3839.0
Crystal size (mm ³)	0.147 × 0.035 × 0.018
Radiation	Cu Kα (λ = 1.54184)
2θ range for data collection (°)	7.152 to 162.94
Index ranges	-8 ≤ h ≤ 9, -28 ≤ k ≤ 39, -26 ≤ l ≤ 26
Reflections collected	17906
Independent reflections	17906 [R _{sigma} = 0.0607]
Data/restraints/parameters	17906/192/412
Goodness-of-fit on F ²	1.039
Final R indexes [I ≥ 2σ (I)]	R ₁ = 0.1366, wR ₂ = 0.3464
Final R indexes [all data]	R ₁ = 0.1903, wR ₂ = 0.3926
Largest diff. peak/hole (eÅ ⁻³)	3.37/-3.07

unprecedented 2, 4, 5-tri(*N*-methyl-4-pyridinium)-1, 3-thiazole heterocycle which crystallizes in a complex network of polyiodides and co-crystallized cyclododecasulfur (S₁₂).

2. Experimental

2.1. Synthesis of 1-methyl-4-thiocarbamoylpyridin-1-ium iodide

1-Methyl-4-thiocarbamoylpyridin-1-ium iodide was prepared via a modification of previous literature method [17]. Methyl iodide (0.57 g, 4 mmol) was added in drops to 5.00 mL of dry acetonitrile (CH₃CN) solution of 4-pyridinethioamide (0.50 g, 4 mmol). This caused a colour change from yellow to deep orange as the mixture was stirred for 30 mins at room temperature and followed by reflux for another 10 mins. The mixture was cooled and the precipitate was filtered, cooled and washed thrice with cold CH₃CN and afterwards recrystallized from boiling 99 % ethanol to afford hygroscopic crystals which were stored in a well-sealed flask. Yield: 0.21 g (35 %). M.p.: 219.3-220.9 °C [Lit. 220 °C [18]]. ¹H NMR (D₂O, 300 MHz, δ, ppm): 8.84 (d, 2H Ar, *J* = 6.9 Hz), 8.23 (d, 2H Ar, *J* = 6.9 Hz), 4.38 (s, 3H, N-CH₃).

2.2. Synthesis of compound 1

The reaction that unexpectedly produced **1** used a modification of a published procedure for the synthesis of 3,5-diaryl-1,2,4-dithiazolium triiodides [19]. 1-methyl-4-thiocarbamoyl pyridin-1-ium iodide (0.10 g, 0.65 mmol) and iodine (0.20 g, 0.653 mmol) in 1 mL glacial acetic acid were heated to boil for about 15 minutes. The colour changed to deep red as the reaction progressed. On cooling, a black-purple precipitate began to form in the acetic acid, which was collected by filtration and thereafter pumped for an extended time under high vacuum. NMR and IR spectroscopic analysis indicated the presence of more than one product but all attempts to separate the bulk mixture failed. Needle-like dark crystals were detected in the solid along with lighter orange and red material. The dark crystals were eventually identified by X-ray crystallography.

2.3. Single crystal structure determination of compound 1

Single crystals of C₂₁H₂₁I₁₃N₄S_{5.98} (**1**) were obtained as dark purple needles by cooling of the reaction mixture. A suitable crystal was selected, mounted on a 100 mm MiTeGen polymer loop in Paratone™ oil and data was collected on a SuperNova Dual, Cu at home/near, Pilatus 200K diffractometer under the control of CrysAlisPro 1.171.41.67a, including integration, scaling and absorption correction using ABSPACK. The crystal was kept at 100.01(10) K during data collection. Using Olex2 [20] the structure was solved with the SHELXT [21] structure solution program using Intrinsic Phasing and refined with the SHELXL [22] refinement package using Least Squares minimization. Twinning was detected during data analysis and refined as a two-component model in a 0.563(4)/0.437(4) ratio. The occupancy of the (half) molecule of S₁₂ was refined using a free variable to an average of 0.83(2) of that of the other components. No evidence of low occupancy for iodine/iodide components could be detected during data refinement. The crystal structure of **1** was analyzed using Mercury software version 4.0.0 [23] and CrystalExplorer 17.5 [24]. The full crystal data have been deposited with the Cambridge Structural Database under CCDC 2056721. Crystal and structure determination parameters are provided in Table 1 and selected interatomic distances and angles in Table 2. The asymmetric unit is shown in a displacement ellipsoids plot in Figure 1 and a unit cell packing diagram in Figure 2.

3. Results and discussion

3.1. Synthesis and product identification

During the attempted synthesis of 3,5-di-(4-pyridyl)-1,2,4-dithiazolium salts by condensation of thioamides, which requires a net oxidation, an attempt was made to stabilize the reactive pyridine groups by alkylation [16]. Thus, the iodide salts of (4-methylpyridyl)thioamide was reacted with elemental iodine as a mild oxidizing agent in hot glacial acetic acid according to standard protocols (Scheme 1, top branch) [19]. The reaction resulted in a complex mixture that included some black needle crystals which could not be identified by spectroscopic techniques.

Table 2. Selected interatomic distances (Å) and angles (°) in structure **1**.

Atom – Atom	Distance	Average ^a	Atom – Atom – Atom	Angle
S1-C1	1.72(3)	1.730(6)	C2-S1-C1	88.4(18)
S1-C2	1.65(4)	1.728(9)	C1-N1-C3	106(3)
N1-C1	1.38(5)	1.310(5)	N1-C1-S1	116(3)
N1-C3	1.42(5)	1.379(4)	N1-C1-C4	120(3)
C2-C3	1.33(5)	1.376(7)	C4-C1-S1	124(2)
C1-C4	1.43(5)	1.471(5)	C2-C2-C1	115(3)
C2-C10	1.54(5)	1.471(3)	C3-C2-C10	126(4)
C3-C16	1.49(5)	1.472(5)	C10-C2-S1	118(3)
I1-I2	2.964(4)		N1-C3-C16	113(3)
I2-I3	2.882(4)		C2-C3-N1	114(3)
$\Delta d(I-I)$ ^a	0.082(3)		C2-C3-C16	132(3)
I4-I5	2.822(4)		S6E ⁱ -S1E-S2E	104.9(9)
I5-I6	3.092(4)		S3E-S2E-S1E	105.9(9)
$\Delta d(I-I)$ ^a	0.269(3)		S4E-S3E-S2E	105.6(10)
I8-I9	2.788(4)		S3E-S4E-S5E	106.2(11)
I10-I11	2.762(5)		S6E-S5E-S4E	105.7(10)
I12-I13	2.756(4)		S5E-S6E-S1E ⁱ	105.5(10)
S1E-S2E	2.06(2)		I3-I2-I1	174.27(13)
S1E-S6E ⁱ	2.05(2)		I4-I5-I6	177.69(13)
S2E-S3E	2.03(2)		I9-I8-I7	
S3E-S4E	2.03(2)			
S4E-S5E	2.06(2)			
S5E-S6E	2.01(2)			

^a Deviation of triiodide bonds from fully symmetrical, defined as $\Delta d(I-I) = |d(I_{\text{term}1}-I_{\text{centr}}) - (I_{\text{term}2}-I_{\text{centr}})|$ Å.

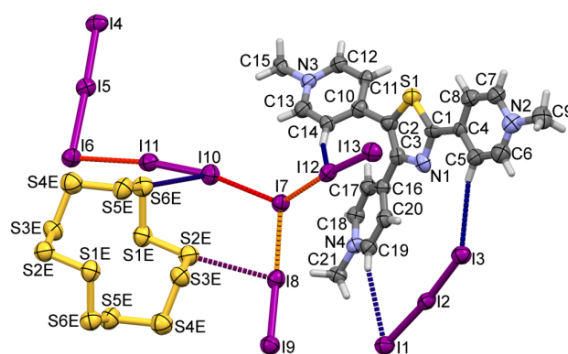


Figure 1. Displacement ellipsoid plot (50% probability) of compound **1** showing the atom labelling scheme. Arbitrarily small radii are used to draw H-atoms for clarity. Short contacts involving iodine are indicated by dashed lines and are coded from the shortest (orange color) to the longest (blue). The S₁₂ molecule has $\bar{1}$ site symmetry; symmetry code i: -x, 1-y, 1-z.

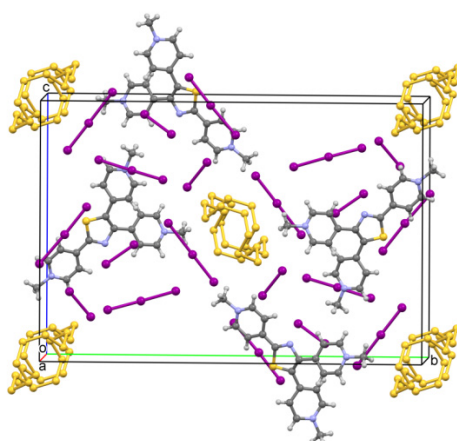
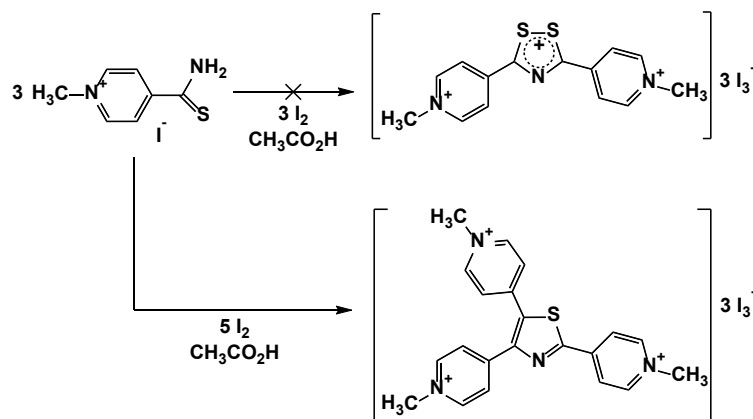


Figure 2. A unit cell packing diagram for compound **1** viewed down the *a* axis. The locations of the S₁₂ molecules at 10 corner and A-face $\bar{1}$ sites in *P2₁/c* defines columns of these almost spherical sulfur molecules through the crystal lattice.

More recently, the availability of a powerful Rigaku-Oxford Diffraction SuperNova diffractometer equipped with a bright microfocus CuK α source and hybrid pixel array detector enabled data collection, structure solution and refinement despite poor crystal quality and the presence of non-merohedral twinning. Surprisingly, the structure determined from crystals of compound **1** shows the presence of iodide/triiodide salts of an unprecedented 2,4,5-tri(*N*-methyl-4-

pyridinium)-1,3-thiazole from a non-oxidative condensation of three equivalents of 4-methylpyridylthioamide iodide, indicating that the actual course of the reaction followed the lower branch of Scheme 1. The structure (Figure 1) is further complemented by the presence of additional iodine molecules and, most surprisingly, by a half-equivalent of cyclododeca sulfur (S₁₂) crystallized at the center of symmetry within the *P2₁/c* lattice.



Scheme 1. Reaction scheme for the formation of the 1,3-thiazole in the structure of compound 1.

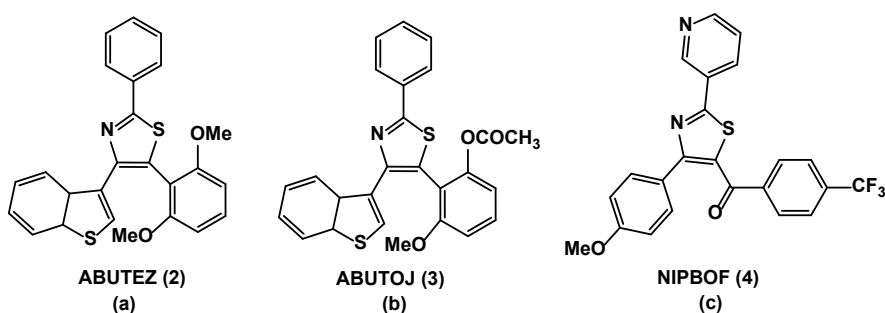


Figure 3. CSD structural comparison with the 1,3-thiazole in the structure of compound 1.

The overall refined occupancy of this S_{12} moiety was determined to be 0.83(2). In view of this complexity, the inability to identify the product using spectroscopic methods is now obvious, and this shows again the power of single-crystal X-ray crystallography as a key analytical tool for synthetic chemistry.

3.2. Structure description

The structure quality of **1** is limited, in part because of the poor crystal quality associated with partial vacancies of co-crystallized S_{12} , but also by the inherent challenge of determining the coordinates of the light-atom organic cation in the presence of thirteen heavy iodine atoms. There is a noticeable lower accuracy in light atom intermolecular distances and angles compared to relatively precise determination of intra- and inter-molecular parameters for the iodine/polyiodide counter-ion assembly.

An important feature of the crystal packing (see [Figure 2](#)) is that the S_{12} molecules occupy columns parallel to the crystal a axis, along the unit cell edges and also the cell centroid. This kind of arrangement is also often seen for solvent molecules, and helps to explain the non-integral occupancy that leads to the lower refined occupancies of these S atoms. We can understand that the lattice energy is primarily defined by the strong tri-cation - anion interactions, allowing the lattice to survive despite the reduced S_{12} occupancies.

The heterocyclic trication found in compound **1** is unique as the first structurally characterized 1,3-thiazole bearing three benzenoid substituents and the first with quaternized 4-pyridinium groups. Some 330 1,3-thiazoles with some form of carbon substituent at each of the 2, 4, and 5 ring positions have been deposited in the CSD. Within this group, there are fourteen structures with two benzenes or azobenzenes in the 1,4-, 10 in 1,5- and thirteen with such groups in 4,5-positions. The closest analogs ([Figure 3](#)) to the trication in compound **1** may be the

photo triggers 4-(1-benzothiophen-3-yl)-5-(2,6-dimethoxyphenyl)-2-phenyl-1,3-thiazole (CSD Refcode: ABUTEZ) (**2**) and 2-(4-(1-benzothiophen-3-yl)-2-phenyl-1,3-thiazol-5-yl)-3-methoxyphenyl acetate (Refcode: ABUTOJ) (**3**) [25], or (4-(4-methoxyphenyl)-2-(pyridin-3-yl)-1,3-thiazol-5-yl)(4-(trifluoromethyl)phenyl)methanone (Refcode: NIPBOF) (**4**) [26]. In the former two, a third substituent is a benzothiophene, and in the latter a phenylketone. In this comparison group, wherein compound **2** is the only one with two independent molecules, we exclude derivatives with fused rings or alkyl substituents, which represent the majority of the extant structures.

Worthy of mention amongst the latter class are the series of ten conformers of the thiazole-based anticancer drug dabrafenib reported by Rai *et al.* (refcodes ZOYXET, ZOYZAR) [27]. Dabrafenib contains a 2-aminopyrimidine ring as one of the thiazole substituents, which in some of these structures is protonated.

In compound **1**, the pyridinium ring attached to the C_1 carbon (2-position) is almost co-planar with the thiazole ring (dihedral angle of $4(2)^\circ$) while those at C_3 (4-position) and C_2 (5-position) twist away from the plane by $28.2(12)^\circ$ and $45.2(9)^\circ$, respectively. In the compound **2**, 1-benzothiophen-3-yl ring, the system twists from the plane by 36.5° and the 2,6-dimethoxyphenyl ring by 44.4° . Compound **3** on the other hand, had a greater twist of 50.2° for the 1-benzothiophen-3-yl ring and 62.7° for the 3-methoxyphenylacetate ring. Compound **4** possesses twists that are intermediate between those of compounds **2** and **3** and greater than what is observed in compound **1** with the pyridine-3-yl at ring position 2 twisting from the plane of the 1,3-thiazole by 13.0° , the 4-methoxyphenyl at position 4 by 49.3° , and the 4-(trifluoromethyl)phenyl)methanone at position 5 by 49.8° . At the 99 % confidence level, the C_1 - C_4 bond distance range of 1.46-1.48 Å in compound **1** aligns with those of compounds **2**, **3**, and **4** within the limit of experimental error ([Table 3](#)).

Table 3. Comparison of selected interatomic distances (Å) and angles (°) in structures **1** – **4**^a.

Atom-atom	1 ^{average}	2'	2''	3	4
C1-S1	1.71 - 1.75	1.72 - 1.74	1.73 - 1.74	1.73 - 1.731	1.72 - 1.73
C2-S2	1.70 - 1.75	1.73 - 1.75	1.72 - 1.73	1.72 - 1.721	1.72 - 1.73
C1-N1	1.30 - 1.32	1.30 - 1.32	1.37 - 1.39	1.30 - 1.31	1.31 - 1.32
C3-N1	1.37 - 1.39	1.37 - 1.39	1.37 - 1.39	1.37 - 1.38	1.37 - 1.38
C2-C3	1.36 - 1.39	1.36 - 1.39	1.36 - 1.38	1.37 - 1.38	1.38 - 1.39
C1-C4	1.46 - 1.48	1.47 - 1.49	1.46 - 1.48	1.46 - 1.47	1.46 - 1.47
C3-C16	1.46 - 1.48	1.45 - 1.48	1.46 - 1.49	1.47 - 1.473	1.47 - 1.49
C2-C10	1.46 - 1.48	1.45 - 1.48	1.46 - 1.49	1.47 - 1.48	1.46 - 1.50
Atom-atom-atom	1 ^{average}	2'	2''	3	4
C1-N1-C3	106(3)	111.2(3)	110.8(3)	110.9(1)	111.1(2)
C2-S1-C1	88.4(18)	89.9(2)	89.9(2)	90.06(7)	89.4(1)
N1-C1-S1	116(3)	114.3(2)	114.4(2)	114.3(1)	115.0(2)
C2-C3-N1	114(3)	115.9(3)	115.9(3)	115.6(1)	114.5(2)
C10-C2-S1	115(3)	108.6(2)	109.0(2)	109.2(1)	109.9(2)
N1-C1-C4	120(3)	118.4(3)	118.9(3)	119.5(3)	123.0(2)
C4-C1-S1	124(2)	122.0(2)	122.1(2)	122.1(1)	122.0(2)
N1-C3-C16	114(3)	122.0(2)	124.0(3)	123.6(1)	118.0(2)
C10-C2-S1	118(3)	121.3(2)	121.7(2)	122.6(1)	116.3(2)
C3-C2-C10	126(4)	125.7(3)	125.1(3)	124.8(1)	127.4(2)
C2-C3-C16	132(3)	129.9(3)	129.9(3)	128.2(3)	133.8(2)

^a All bond lengths were calculated at the 99 % confidence level.

Table 4. Comparison of key geometrical values for the reported crystal structures of S₁₂.

S ₁₂ molecules	S-S _{Average} (Å)	∠S-S-S _{Average} (°)	Torsion angle (°)	Reference
S ₁₂ as found in 1 ^a	2.040(18)	105.6(4)	88(2)	This work
S ₁₂ ^b	2.052	106.6	88.00	[29]
S ₁₂ .CS ₂ ^c	2.054	105.8	87.20	[29]
S ₁₂ ^b	2.055	106.5	88.00	[28]

^a P2₁/c with $\bar{1}$ site symmetry.

^b Pnnm with D_{2h} site symmetry.

^c R3m with D_{3d} site symmetry.

In general, the low precision of the cation geometry observed in compound **1** results in interatomic distances and angles that are broadly comparable with and statistically indistinguishable from the comparison structures.

The neutral S₁₂ molecule, which is centrosymmetric and displays the approximate D_{3d} conformation observed previously, is the second most thermodynamically stable allotrope of sulfur after S₈. The S atoms are located in three parallel planes, a central plane of six atoms (S1E, S5E, S6E) and upper and lower planes of three each (S2E, S3E and S4E). The source of all sulfur in this reaction is the thioamide, but the condensation reaction (Scheme 1) accounts stoichiometrically for only two of the six excess sulfur atoms detected in the lattice of compound **1**. Hence, the low yield of compound **1** is unsurprising. Interestingly, to the best of our knowledge, this is the first report of thioamides as a sulfur source for cyclododecasulfur (S₁₂) [15]. To date, very few reports of the crystal structure of S₁₂ have been published. The first publication by Kutoglu et al. reported S₁₂ with two molecules in the asymmetric unit [28], while close to two decades later, Steidel *et al.* improved on the refinement of this S₁₂ structure and also reported a 1:1 S₁₂/CS₂ co-crystal [29]. The structure of S₁₂ in **1** compound displays quite comparable average S-S distances, S-S-S angles and torsions (Table 4). As expected from crystallization with only $\bar{1}$ site symmetry, the structural features of compound **1** have lower overall symmetry than the previously reported structures. Thus, the consistency of the geometry of S₁₂ in compound **1** provides important confirmation of this known geometry, which has also been supported by computational studies [15].

3.3. Lattice structure and short intermolecular contacts

As might be expected for a 3+ charged cation salt structure such as compound **1**, numerous intermolecular interactions are present and these include short contacts such as I...I, I...S, I...C and C...S coupled with quite a number of weak C-H...I and C-H...S non-classical hydrogen bond interactions; a discussion of the latter follows in the next section using Hirshfeld surfaces. We focus here on the most important contacts which have contact distances shorter than 0.1 less than the sum of the van der Waals

radii of the contacting atoms (Table 5). These are also depicted in Figure 1 as dashed lines colored by contact strength. The vast majority of the strong contacts involve the neutral and anionic iodine atoms, interacting with other iodine, with sulfur in S₁₂, and to a lesser extent with C-H and possibly with C directly in the methyl group of C15.

The +3 charge from the three methylated pyridyl rings necessitated neutralization by three triiodide counterions. Interactions of I₂ with unsaturated nitrogen-containing heterocycles are likely to result in very complex combinations of molecules and ions [9,13]. Iodine-rich complex salts (polyiodides) are increasingly recognized in which iodides and especially triiodides salts are capable of forming compounds of higher iodine content by coordinating with I₂ molecules [9,12]. As shown in Figure 2, I1-I3 and I4-I6 exist in the lattice as fairly distinct triiodides, the former quite symmetrical with $\Delta d(I-I) = 0.082(3)$ and the latter less so with $\Delta d(I-I) = 0.269(3)$ Å (Table 2). The I₃⁻ is readily polarized resulting in different bond lengths for the I-I bonds. However, if the cation is relatively large, then the I-I bonds remain closely symmetrical in the I₃⁻ [30]. The asymmetry for I7-I9 is extreme ($\Delta d(I-I) = 0.400(3)$ Å) and we prefer a description of I7⁻ as iodide complexed by three iodine molecules, I8-I9 {3.188(4) Å}, I10-I11 {3.316(4) Å} and I12-I13 {3.485(4) Å}, with the indicated interatomic contact distances (see Table 5) that range from 0.77 to 0.48 Å less than the sums of the van der Waals' radii of two iodine atoms. The geometry at I7 is between "T-shaped" and trigonal pyramidal with close-to-linear I₂/I⁻ arrays and the sums of angles at I7 of 347.5(2)°. It should be noted that I10-I11 forms a shorter contact to I6 of 3.389(4) Å than to I7, resulting in an "L-shaped" interaction with an angle of 93.1°. On this description, the three predominantly I₂ molecules have bonds ranging from 2.756(4) to 2.788(4) Å, in reasonable agreement with 2.72 Å found in elemental iodine [31] and longer than 2.66 Å for I₂(g) [32].

3.4. Hirshfeld Analysis of compound **1**

The Hirshfeld surface (HS) mapped over a 3D electrostatic potential (ESP) surface at the Tonto-sourced HF/STO-3G level of theory in the range -0.0945 au (red) through 0.0 (white) to

Table 5. Important intermolecular contacts other than non-classical H-bonds in the structure **1**^a.

Atom 1	Atom 2	Length	Length - $\sum r_{(vdW)}$	Symmetry code ^b
I7	I8	3.188(4)	-0.773	-
I7	I12	3.316(4)	-0.644	-
I6	I11	3.389(4)	-0.571	-
I7	I10	3.485(4)	-0.475	-
I13	I11	3.647(4)	-0.313	x,1.5-y,1/2+z
I9	I6	3.660(4)	-0.300	1-x,1-y,1-z
C15	I12	3.47(4)	-0.205	x,1.5-y,-1/2+z
I8	S2E	3.590(16)	-0.192	-
I10	S4E	3.662(18)	-0.117	1-x,1-y,1-z

^a Contacts shorter than 0.1 Å less than sums of the van der Waals radii of the contacting atoms.

^b Symmetry operator for Atom 2 in the contact definition.

Table 6. Non-classical Hydrogen Bonds identified by Hirshfeld surfaces mapped on a d_{norm} .

C-H...X	H...X (Å)	C...X (Å)	∠C-H...X (°)
C _{Methyl} -H...I	2.851	3.925	171.56
C _{Methyl} -H...I	2.876	3.719	139.72
C _{Meta-Py} -H...I	2.719	3.762	149.19
C _{Ortho-Py} -H...I	2.860	3.704	134.88
C _{Ortho-Py} -H...I	3.009	3.974	148.60
C _{Ortho-Py} -H...I	3.027	3.997	149.39
C _{Methyl} -H...S	2.547	3.524	149.50
C _{Methyl} -H...Iodine	3.314	3.476	89.33

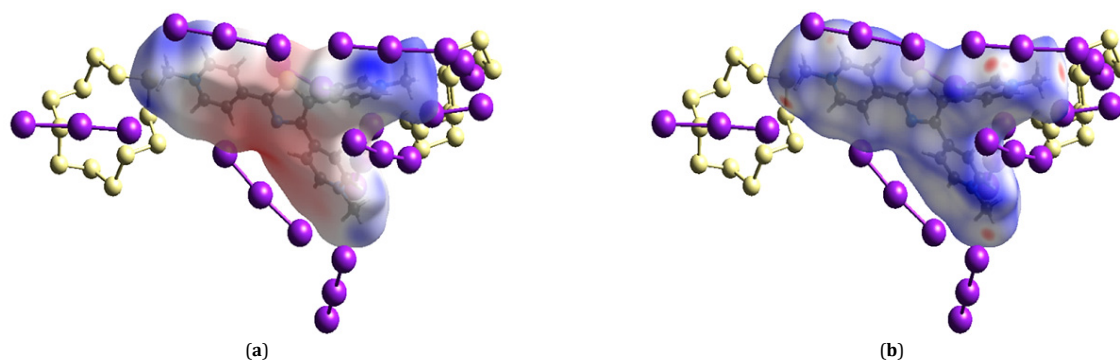


Figure 4. The Hirshfeld surface of compound **1** mapped on: (a) an electrostatic potential showing the negative (red) and positive (blue) ESP regions; (b) a d_{norm} surface showing asymmetrically distributed red hotspots identifying C-H...I and C-H...S non-classical hydrogen bonds whose lengths are less than the sums of the van der Waals radii of the contacting atoms.

0.0538 au (blue) shows very reddish ESP regions over the thiazole ring implying negative charge regions (Figure 4a). Other less reddish ESP regions are over the methylated pyridyl rings at the 1,3,5-positions indicative of the existence of π electrons. Deep blue, positive ESP regions hover on the N-methyl groups and are indicative of their hydrogen donor abilities. It is deemed fit to infer that the positive regions at the $\text{CH}_3\text{-N}^+$ regions are charge acceptors with the eventual formation of some short contacts with iodide, triiodide and from one of the S_{12} sulfur atoms. Therefore, all the 'nearest neighbor' contacts are mainly from the trication, the counter anions, and in just one site to the S_{12} making it reasonable to refer to the blue and red zones as regions of positive and negative charge accumulations.

The HS computed for the structure of compound **1** colored by d_{norm} reveals eight asymmetrical red hotspots that identify interactions with shorter distances than the summation of the van der Waals radii (Figure 4b). The interactions identified (Table 6) by linking components internal to the DFT calculations with external fragments (i.e. I_2 , I_3^- and S_{12}) can all be described as non-classical hydrogen bond interactions (NC-HBI) of the type $\text{C}_{\text{Methyl}}\text{-H}\cdots\text{I}$, $\text{C}_{\text{Ortho-Py}}\text{-H}\cdots\text{I}$, $\text{C}_{\text{Methyl}}\text{-H}\cdots\text{S}$ and $\text{C}_{\text{Meta-Py}}\text{-H}\cdots\text{I}$ and $\text{C}_{\text{Methyl}}\text{-H}\cdots\text{Iodine}$ in the quantity ratio 2:3:1:1:1 respectively. Interestingly, 2D fingerprint plots (FP) were generated from d_e versus d_i graphs that were generated from HS. Through Fingerprint analysis (Figure 5), quite a number of intermolecular short contacts and NC-HBI were identified and quantified via reciprocal surface areas. The interactions and their reciprocal surface areas are H...S (9.5 %), S...I (3.6 %), N...I

(4.7 %), H...C (0.4 %), C...I (18.1 %), H...H (10.4 %) and H...I (53.2 %). The S...I short contacts in particular are clear pointers to the polarization of the I_3^- with partial negative charge at the I⁻ end and partial positive charge at the central I atom. Based on these outcomes, CrystalExplorer has shown its advantage over the conventional Mercury structure viewer in resolving, identifying and quantifying complex atom-atom interactions especially H...H and N...I. Moreover, in alignment with structural findings using the Mercury structural viewer, CrystalExplorer has revealed the iodine/iodide network as a major determinant in the stability of the crystal lattice of compound **1** based on the high reciprocal surface areas occupied by I-containing contacts and NC-HBI.

4. Conclusion

Here, we report the solid-state identification of an unprecedented 2,4,5-tri(*N*-methyl-4-pyridinium)-1,3-thiazole in a lattice where it forms a complex network of polyiodide/iodine counterions and co-crystallized cyclododecasulfur (S_{12}). Their formation has been revealed to be as a result of chemical/redox condensation and decomposition of starting materials. With the aid of conventional Mercury structural viewer and CrystalExplorer for Hirshfeld surface analysis, it was observed that (1) the crystal lattice is host to a number of stabilizing coulombic short contacts such as I...I, I...S, I...C and C...S and non-covalent interactions such as weak C-H...I and C-H...S NC-HBI and (2) the iodine/iodide network in compound **1** are major determinants in the stability of its crystal lattice.

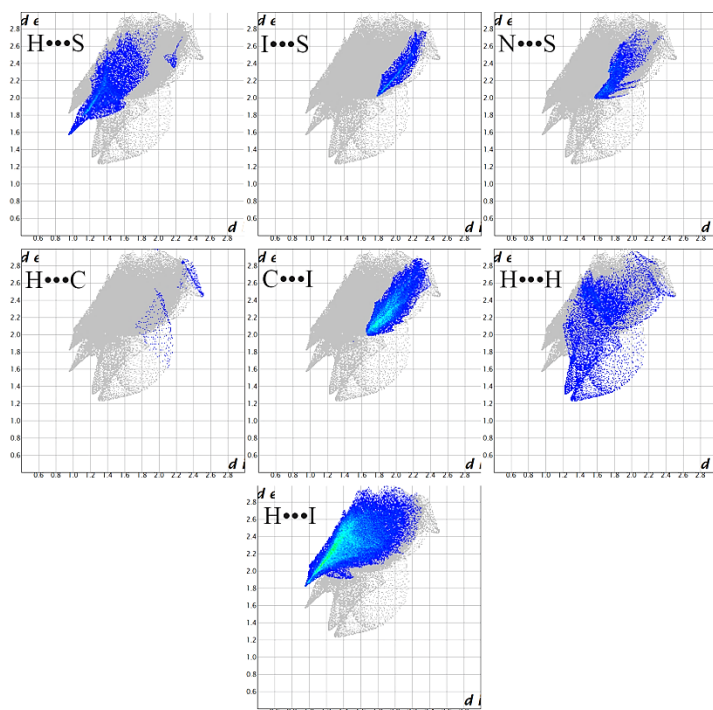


Figure 5. Fingerprint plots identifying intermolecular short contacts and non-classical hydrogen bond interactions.

Acknowledgements

We acknowledge financial support from Lagos State University during Ibukun Oluwaseun Shotonwa's Training Leave. The Natural Sciences and Engineering Research Council of Canada is gratefully acknowledged for Discovery Grants (RTB). We thank the University of Lethbridge and the Faculty of Arts and Science for the purchase of the Rigaku-Oxford Diffraction SuperNova diffractometer.

Supporting information

CCDC-2056721 contains the supplementary crystallographic data for this paper. These data can be obtained free of charge via <https://www.ccdc.cam.ac.uk/structures/>, or by emailing data_request@ccdc.cam.ac.uk, or by contacting The Cambridge Crystallographic Data Centre, 12 Union Road, Cambridge CB2 1EZ, UK; fax: +44(0)1223-336033.

Disclosure statement

Conflict of interests: The two authors declare no conflict of interest.


Author contributions: René T. Boéré solved and refined the crystal structure model as well as reviewed the paper; Ibukun Oluwaseun Shotonwa carried out data analysis and came up with the final drafts of the paper.

Ethical approval: There is adherence to all ethical guidelines.

Sample availability: Samples of the target product are not available from the author.

ORCID

Ibukun Oluwaseun Shotonwa

 <https://orcid.org/0000-0002-5364-717X>

René T. Boéré

 <https://orcid.org/0000-0003-1855-360X>

References

- [1]. Fahim, A. M.; Farag, A. M.; Shaaban, M. R.; Ragab, E. A. *Eur. J. Chem.* **2018**, *9* (1), 30–38.
- [2]. Saroha, M.; Khurana, J. M. *New J Chem* **2019**, *43* (22), 8644–8650.
- [3]. Ripain, I. H. A.; Roslan, N.; Norshahimi, N. S.; Salleh, S. S. M.; Bunnori, N. M.; Ngah, N. *Malays. J. Anal. Sci.* **2019**, *23* (2), 237–246.
- [4]. Xu, Z.; Ba, M.; Zhou, H.; Cao, Y.; Tang, C.; Yang, Y.; He, R.; Liang, Y.; Zhang, X.; Li, Z.; Zhu, L.; Guo, Y.; Guo, C. *Eur. J. Med. Chem.* **2014**, *85*, 27–42.
- [5]. Karale, U. B.; Krishna, V. S.; Krishna, E. V.; Choudhari, A. S.; Shukla, M.; Gaikwad, V. R.; Mahizhaveni, B.; Chopra, S.; Misra, S.; Sarkar, D.; Sriram, D.; Dusthacker, V. N. A.; Rode, H. B. *Eur. J. Med. Chem.* **2019**, *178*, 315–328.
- [6]. Thomae, D.; Perspicace, E.; Xu, Z.; Henryon, D.; Schneider, S.; Hesse, S.; Kirsch, G.; Seck, P. *Tetrahedron* **2009**, *65* (15), 2982–2988.
- [7]. Luqman, A.; Blair, V. L.; Brammananth, R.; Crellin, P. K.; Coppel, R. L.; Andrews, P. C. *Eur. J. Inorg. Chem.* **2016**, *2016* (17), 2738–2749.
- [8]. Shahbazi-Raz, F.; Amani, V.; Noruzi, E. B.; Safari, N.; Boča, R.; Titiš, J.; Notash, B. *Inorg. Chim. Acta* **2015**, *435*, 262–273.
- [9]. Rimmer, E. L.; Bailey, R. D.; Pennington, W. T.; Hanks, T. W. *J. Chem. Soc., Perkin Trans. 2* **1998**, No. 11, 2557–2562.
- [10]. Danten, Y.; Guillot, B.; Guissani, Y. *J. Chem. Phys.* **1992**, *96* (5), 3795–3810.
- [11]. Blake, A.; Li, W.-S.; Lippolis, V.; Schröder, M.; A. Devillanova, F.; O. Gould, R.; Parsons, S.; Radek, C. *Chem. Soc. Rev.* **1998**, *27* (3), 195–205.
- [12]. Savastano, M.; Bazzicalupi, C.; Gellini, C.; Bianchi, A. *Crystals (Basel)* **2020**, *10* (5), 387–400.
- [13]. Wang, Y.; Xue, Y.; Wang, X.; Cui, Z.; Wang, L. *J. Mol. Struct.* **2014**, *1074*, 231–239.
- [14]. Bailey, R. D.; Pennington, W. T. *Acta Crystallogr. B* **1995**, *51* (5), 810–815.
- [15]. Steudel, R.; Eckert, B. Solid Sulfur Allotropes Sulfur Allotropes. In *Elemental Sulfur and Sulfur-Rich Compounds I*; Springer Berlin Heidelberg: Berlin, Heidelberg, 2012; pp 1–80.
- [16]. Shotonwa, I. O.; Boéré, R. T. *IUCrdata* **2018**, *3* (11), 3, 181491–181493.
- [17]. Kosower, E. M. *J. Am. Chem. Soc.* **1955**, *77* (14), 3883–3885.
- [18]. Christ, W.; Rakow, D.; Strauss, S. J. *Heterocycl. Chem.* **1974**, *11* (3), 397–399.
- [19]. Liebscher, J.; Hartmann, H. *Justus Liebigs Ann. Chem.* **1977**, *1977* (6), 1005–1012.
- [20]. Dolomanov, O. V.; Bourhis, L. J.; Gildea, R. J.; Howard, J. A. K.; Puschmann, H. *J. Appl. Crystallogr.* **2009**, *42* (2), 339–341.
- [21]. Sheldrick, G. M. *Acta Crystallogr. A Found. Adv.* **2015**, *71* (Pt 1), 3–8.
- [22]. Sheldrick, G. M. *Acta Crystallogr. C Struct. Chem.* **2015**, *71* (Pt 1), 3–8.

- [23]. Macrae, C. F.; Bruno, I. J.; Chisholm, J. A.; Edgington, P. R.; McCabe, P.; Pidcock, E.; Rodriguez-Monge, L.; Taylor, R.; van de Streek, J.; Wood, P. A. *J. Appl. Crystallogr.* **2008**, *41* (2), 466–470.
- [24]. Turner, M. J.; McKinnon, J. J.; Wolff, S. K.; Grimwood, D. J.; Spackman, P. R.; Jayatilaka, D.; Spackman, M. A. *CrystalExplorer17*; University of Western Australia, 2017.
- [25]. Galangau, O.; Delbaere, S.; Ratel-Ramond, N.; Rapenne, G.; Li, R.; Calupitan, J. P. D. C.; Nakashima, T.; Kawai, T. *J. Org. Chem.* **2016**, *81* (22), 11282–11290.
- [26]. Pampa, K. J.; Abdoh, M. M. M.; Swaroop, T. R.; Rangappa, K. S.; Lokanath, N. K. *Acta Crystallogr. Sect. E Struct. Rep. Online* **2013**, *69* (Pt 9), o1434.
- [27]. Rai, S. K.; Gunnam, A.; Mannava, M. K. C.; Nangia, A. K. *Cryst. Growth Des.* **2020**, *20* (2), 1035–1046.
- [28]. Kutoglu, A.; Hellner, E. *Angew. Chem. Int. Ed. Engl.* **1966**, *5* (11), 965–965.
- [29]. Steidel, J.; Steudel, R.; Kutoglu, A. *Z. Anorg. Allg. Chem.* **1981**, *476* (5), 171–178.
- [30]. Atkins, P. W. S.; Atkins'. *Inorganic Chemistry*; Oxford University Press: Oxford; New York, 2010.
- [31]. Batsanov, S. S. *Inorg. Mater.* **2001**, *37* (9), 871–885.
- [32]. Sütay, B.; Yurtsever, M.; Yurtsever, E. *J. Mol. Model.* **2014**, *20* (10), 2445–2454.



Copyright © 2021 by Authors. This work is published and licensed by Atlanta Publishing House LLC, Atlanta, GA, USA. The full terms of this license are available at <http://www.eurjchem.com/index.php/eurjchem/pages/view/terms> and incorporate the Creative Commons Attribution-Non Commercial (CC BY NC) (International, v4.0) License (<http://creativecommons.org/licenses/by-nc/4.0>). By accessing the work, you hereby accept the Terms. This is an open access article distributed under the terms and conditions of the CC BY NC License, which permits unrestricted non-commercial use, distribution, and reproduction in any medium, provided the original work is properly cited without any further permission from Atlanta Publishing House LLC (European Journal of Chemistry). No use, distribution or reproduction is permitted which does not comply with these terms. Permissions for commercial use of this work beyond the scope of the License (<http://www.eurjchem.com/index.php/eurjchem/pages/view/terms>) are administered by Atlanta Publishing House LLC (European Journal of Chemistry).